Journal of Power Sources 196 (2011) 10782–10787

Contents lists available at SciVerse ScienceDirect

Journal of Power Sources

journal homepage: www.elsevier.com/locate/jpowsour

Graphene–MnO_2 and graphene asymmetrical electrochemical capacitor with a high energy density in aqueous electrolyte

Lingjuan Deng, Gang Zhu, Jianfang Wang, Liping Kang, Zong-Huai Liu*, Zupei Yang, Zenglin Wang

Key Laboratory of Applied Surface and Colloid Chemistry (Shaanxi Normal University), Ministry of Education, Xi'an 710062, PR China

ARTICLE INFO

Article history:
Received 13 June 2011
Received in revised form 6 August 2011
Accepted 2 September 2011
Available online 10 September 2011

Keywords:
Hybrid material
Asymmetric electrochemical capacitor
Energy density
Cycle stability

ABSTRACT

The graphene–manganese oxide hybrid material has been prepared by solution-phase assembly of aqueous dispersions of graphene nanosheets and manganese oxide nanosheets at room temperature. The morphology and structure of the obtained material are examined by scanning electron microscopy, transition electron microscopy, X-ray diffraction and N_2 adsorption–desorption. Electrochemical properties are characterized by cyclic voltammetry, galvanostatic charge–discharge and electrochemical impedance spectroscopy. An asymmetric electrochemical capacitor with high energy and power densities based on the graphene–manganese oxide hybrid material as positive electrode and graphene as negative electrode in a neutral aqueous Na_2SO_4 solution as electrolyte is assembled. The asymmetrical electrochemical capacitor could cycle reversibly in a voltage of 0–1.7 V and give an energy density of 10.03 Wh kg^{-1} even at an average power density of 2.53 kW kg^{-1}. Moreover, the asymmetrical electrochemical capacitor exhibit excellent cycle stability, and the capacitance retention of the asymmetrical electrochemical capacitor is 69% after repeating the galvanostatic charge–discharge test at the constant current density of 2230 mA g^{-1} for 10,000 cycles.

1. Introduction

Electrochemical capacitors have attracted considerable attention over the past decades because of their high power density and long cycle life, and they can be used as the assistant and buffering systems for several primary power sources (e.g., electric vehicles, hybrid electric vehicles, and many typical stop-and-go systems) and the renewable energy generation systems [1–3]. According to the charge storage mechanism, electrochemical capacitors can be generally divided into three categories, they are double-layer capacitors (EDLC), pseudocapacitors and hybrid-type asymmetric electrochemical capacitors [4]. The research results show that the capacity performance of the electrochemical capacitors is connected with the active electrode materials [5]. Up to now, porous carbon, conducting polymers, and transition-metal oxides are promising candidates for the electroactive materials of electrochemical capacitors [6–8], but each kind of these materials has its own advantages and disadvantages. Porous carbon materials show long cycle life and good mechanical properties, but the specific capacitance is low [9], while conducting polymers have high flexibility and good cycle performance in a suitable potential window of charge storage/delivery [6,10]. Among the transition-metal oxides, manganese oxides have received tremendous attention for electrochemical capacitors due to its low cost, abundance, high theoretical specific capacitance (1100 F g^{-1}) and good environmental compatibility [11]. Moreover, a hierarchical nanostructure consisting of amorphous MnO_2, Mn_3O_4 nanocrystallites, and single-crystalline MnOOH nanowires shows excellent capacitance retention (96%) after 10,000 cycles of charge–discharge test [12].

Nowadays, commercial electrochemical capacitors are mainly based on two symmetrical active carbon electrodes separated by a cellulosic or a polymeric membrane impregnated with an organic salt electrolyte [13]. Although active carbon electrochemical capacitors exhibit long cycle life, the power and energy densities are need to be improved [14]. To solve this problem, asymmetric (hybrid) systems have been extensively explored by combining a battery-like Faradic electrode (as energy source) and a capacitive electrode (as power source) to increase the operation voltage, which leads to a notable improvement of the energy density of high-power electrochemical capacitors so that it approaches that of batteries [15–18]. Many asymmetric electrochemical capacitors have been assembled by using MnO_2, Fe_3O_4, NiO and WO_3–$WO_3{\cdot}0.5H_2O$ as the positive electrode and the active carbon, conducting polymer or $RuO_2{\cdot}xH_2O$ as the negative electrode [4,19–21]. For example, an asymmetrical electrochemical capacitor (MnO_2 is positive electrode and active carbon is negative electrode) has been cycled between 0 and 2.2 V at the constant power density (1.2 kW kg^{-1}) over 10,000 cycles, but a constant fade in energy density is observed upon cycling, and

* Corresponding author at: School of Chemistry and Materials Science of Shaanxi Normal University, Xi'an, Shaanxi 710062, PR China. Tel.: +86 29 85303701; fax: +86 29 85307774.
E-mail address: zhliu@snnu.edu.cn (Z.-H. Liu).

0378-7753/$ – see front matter © 2011 Elsevier B.V. All rights reserved.
doi:10.1016/j.jpowsour.2011.09.005

only 55% of the initial energy density is retained after 10,000 cycles [19].

Graphene is considered to be the most potential electrical double-layer capacitors material due to its high electrical conductivity, good electrochemical stability, high surface area and superior mechanical property [22]. However, the actual capacitive behavior of pure graphene is much lower than the anticipated value due to the fact that it usually suffers from serious agglomeration during preparation [23]. It has been found that the capacitance of graphene can be improved by combining with some pseudocapacitive electrode materials, such as conducting polymers and transition-metal oxides [24–28], and several kinds of graphene–manganese oxide composites with good capacitance performance have been prepared by the surface redox reaction and electrodeposition methods [23,25–27]. Manganese oxide nanosheets have not only distinctive physicochemical properties, associated with dimensions in the nanometer range, but also large surface area. They can be obtained through the delamination of the layered MnO_2, and can be employed as a new class of nanoscale materials [29]. Sophisticated functionalities or nanodevices may be designed through the selection of nanosheets and combining materials, and precise control over their arrangement at the molecular scale [30,31]. Therefore, the hybrid material obtained from manganese oxide nanosheets and graphene is expected to be prepared. By using this hybrid material, asymmetric electrochemical capacitors which give high power and energy densities could be assembled.

In this paper, graphene–MnO_2 hybrid material is prepared by solution-phase assembly of aqueous dispersions of graphene nanosheets and manganese oxide nanosheets at room temperature. On the basis of the graphene–MnO_2 hybrid material and graphene, an asymmetrical electrochemical capacitor is assembled, with 1 M Na_2SO_4 solution as the electrolyte. The asymmetrical electrochemical capacitor can cycle reversibly in a voltage of 0–1.7 V and give an energy density of 10.03 Wh kg^{-1} even at an average power density of 2.53 kW kg^{-1}. Moreover, it has reasonable cycling performance.

2. Experimental

2.1. Materials synthesis

Crude flake graphite (carbon content: 99.9%) was purchased from Qingdao Aoke Co., tetramethylammonium hydroxide (TMAOH, 25 wt.%) was purchased from Alfa Aesar Co. $Mn(NO_3)_2$ (50%), NaOH, H_2O_2 (30%), H_2SO_4 (98%), $KMnO_4$, $K_2S_2O_8$, P_2O_5, HCl (37%), hydrazine solution (50%) and ammonia solution (25%) were obtained from Chemical Reagent Ltd., China, in the analytical purity and used without further purification. Deionized water was used throughout the experiments.

Graphite oxide (GO) was fabricated from crude flake graphite by a modified Hummers method [32]. The as-prepared GO was then treated by ultrasonication treatment using a KQ-600kDE Digital Ultrasonic cleaning device (600 W, 80% amplitude) in a water bath for an hour, and GO homogeneous dispersion (0.25 mg mL^{-1}) was obtained. The GO homogeneous dispersion (100 mL) was mixed with hydrazine solution (35 μL) and ammonia solution (400 μL), followed by stirring for 10 min. The mixture was then heated to 95 °C and stirred for an hour, GO was reduced to graphene and the stable graphene dispersion was obtained.

Na-type layered manganese oxide was synthesized as reported in the literature [33]. The obtained Na-type layered manganese oxide was treated with a 0.1 M HCl solution at room temperature for 3 days to produce H-type layered manganese oxide, which had a chemical formula of $H_{0.27}MnO_2{\cdot}0.67H_2O$. Delamination of H-type layered manganese oxide was carried out by the method described in the literature [29]. H-type layered manganese oxide (1 g) was treated in a 1.0 M aqueous solution of TMAOH (100 mL) for 7 days at room temperature. After soaking, the colloidal suspension was centrifuged at a speed of 13,000 rpm for 20 min to remove any unexfoliated layered manganese oxide, and then the delaminated layered manganese oxide slurry was obtained.

The graphene–MnO_2 hybrid material was prepared by the following procedures. The pH value of the obtained layered manganese oxide slurry (15 mL) was adjusted to that of the graphene nanosheet dispersion (300 mL), and then two dispersions were mixed and stirred for 7 days at room temperature. The obtained precipitate was filtrated with a nylon membrane (0.22 μm) and freeze-dried for 24 h to obtain the graphene–MnO_2 hybrid material.

2.2. Characterizations

X-ray diffraction (XRD) measurements were carried out using a D/Max2550VB+/PC X-ray diffractometer with Cu Kα (λ = 1.5406 Å), using an operation voltage and current of 40 kV and 40 mA, respectively. A Quanta 200 environmental scanning electron microscope (SEM) was used to observe the morphology of the obtained materials. Transmission electron microscope (TEM) images were collected by using a JEM-2100 microscope working at 200 kV. Specimens for TEM observation were prepared by dispersing the material powder into alcohol by an ultrasonic treatment. A Beckman coulter-type nitrogen adsorption–desorption apparatus (ASAP 2020M) was used to investigate the pore property degassing at 120 °C for 12 h below 10^{-3} mmHg. An IVIUMSTAT electrochemical workstation (Ivium Technologies BV Co., Holland) was used for electrochemical measurements. The Mn content in the hybrid materials was determined by atomic absorption spectrometry after materials were dissolved in a mixed solution of HCl and H_2O_2.

2.3. Electrochemical measurement

Electrodes were prepared by mixing the obtained materials (75 wt.%) as active material with acetylene black (20 wt.%) and polyvinylidene fluoride (5 wt.%). The first two constituents were firstly mixed together to obtain a homogeneous black powder. The polyvinylidene fluoride solution (0.02 g mL^{-1}, in nmethylketopyrrolidine) was then added. This resulted in a rubber-like paste, which was coated on a Ni mesh (typical surfaces: 2 cm^2). The mesh was dried at 110 °C in air for 12 h for the removal of the solvent. After drying, the coated mesh was uniaxially pressed to completely adhere to the electrode material with the current collector. The graphene negative electrode was prepared by the same procedure. To construct an asymmetric electrochemical capacitor, the loading mass ratio of the active material (graphene–MnO_2) to graphene was 0.8.

The cyclic voltammetry (CV) test of the individual electrode was performed in a three-electrode cell, in which platinum-foam (2 cm^2) and a saturated calomel electrode (SCE) were used as counter electrode and reference electrode, respectively, in a 1 M Na_2SO_4 electrolyte. The CV and galvanostatic charge–discharge tests of the symmetric electrochemical capacitor (graphene//graphene, graphene–MnO_2//graphene–MnO_2) and the asymmetric electrochemical capacitor (graphene–MnO_2// graphene) separated by a glass paper fiber were performed in a two-electrode cell in the 1 M Na_2SO_4 electrolyte. The electrode and glass fiber layers were then pressed between two nickel current collectors by the mean of stainless steel clamps.

The specific capacitance C (F g^{-1}), energy density E (Wh kg^{-1}) and average power density P_{av} (W kg^{-1}) of the electrochemical capacitor were determined by means of galvanostatic charge–discharge cycles as follows:

$$C = \frac{It}{(\Delta V)m} \quad (1)$$

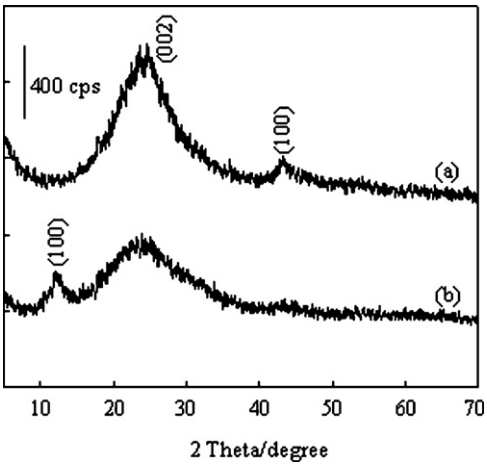

Fig. 1. XRD patterns of the graphene (a) and graphene–MnO_2 hybrid material (b).

$$E = \frac{C(\Delta V)^2}{2 \times 3600} \quad (2)$$

$$P_{av} = \frac{E}{t} \quad (3)$$

where $\Delta V = (V_{max} - V_{min})$, V_{max} is the potential at the end of charge and V_{min} at the end of discharge, m is the active mass of the two composite electrode (kg), I is the applied current (A) and t is the time of discharge stage (s).

3. Results and discussion

The H-type manganese oxide has a layered structure with a basal spacing of 0.73 nm, and it can be delaminated into the individual manganese oxide nanosheets after it is treated with a tetramethylammonium hydroxide (TMAOH) solution for 7 days (Fig. S1) [33]. The delaminated manganese oxide nanosheets have a higher degree of freedom than the stacked nanosheets, the bulky guest ions or polymer molecules can be easily adsorbed onto their surface. When the delaminated manganese oxide nanosheets slurry is mixed with graphene nanosheets dispersion and stirred for 7 days at room temperature, a reassembling reaction between manganese oxide nanosheets and graphene nanosheets is carried out, and the graphene–MnO_2 hybrid material is obtained. The graphene–MnO_2 hybrid material shows similar XRD pattern of the graphene, not only the broad (0 0 2) characteristic diffraction peak due to the stacking of graphene nanosheets can be observed, but also another new peak ($2\theta = 12^\circ$) is indexed, which is ascribed to (0 0 1) diffraction peak of MnO_2 with a layered structure (JCPDS No. 43-1456). The (0 0 1) diffraction peak is broadened, indicating the poor crystallinity of the MnO_2 in the hybrid material (Fig. 1b). According to the atomic absorption analytic result, the amount of MnO_2 in the hybrid material is 18%.

SEM and TEM images of the graphene–MnO_2 hybrid material are shown in Fig. 2. It can be seen that the obtained hybrid material shows two characteristic morphologies, which are large platelike and loose curling morphologies. In addition, no obvious nanosheets aggregation is observed, suggesting graphene nanosheets and manganese oxide nanosheets assemble freely (Fig. 2a). TEM characterization further confirms the intimate contact between the graphene nanosheets and manganese oxide nanosheets, and the loose curling manganese oxide nanosheets are reassembled on the graphene nanosheets (Fig. 2b). Moreover, two kinds of contrast fringes can be observed from high-resolution TEM (HRTEM) (Fig. 2c). The lattice fringe with an interplanar distance of 0.7 nm is ascribed to the (0 0 1) plane of the layered MnO_2, while the 0.3 nm

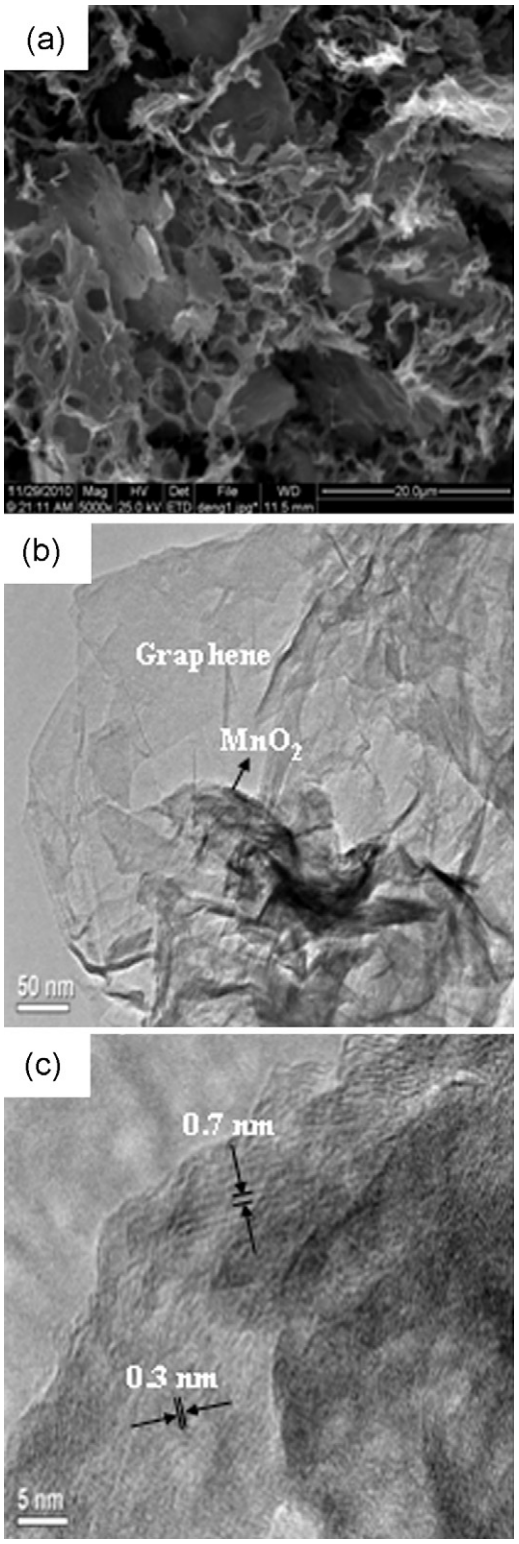

Fig. 2. SEM (a), low-magnification TEM (b), and HRTEM images (c) of the graphene–MnO_2 hybrid material.

is caused by the (0 0 2) plane of the graphene [34]. It is believed that the assembly of curling manganese oxide nanosheets on the surface of graphene nanosheets to some extent prevents the stacking of graphene nanosheets due to van der Waals interactions, leading to a large available surface area and rich porous structure for energy storage. On the other hand, the presence of graphene is favorable to improve the electrical conductivity of the hybrid material [25].

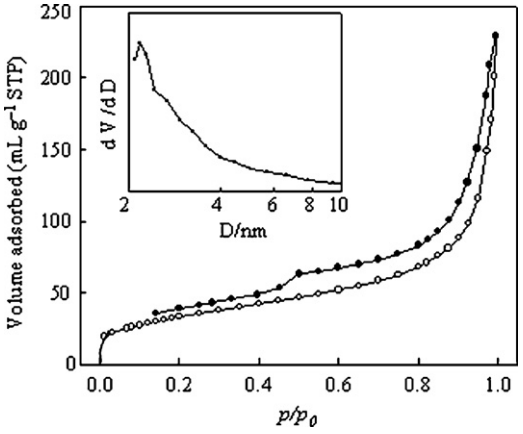

Fig. 3. N_2 adsorption–desorption isotherms and the BJH adsorption pore size distribution (the inset) of the graphene–MnO_2 hybrid material.

Fig. 3 depicts the N_2 adsorption–desorption isotherms and BJH adsorption pore size distribution (inserted in Fig. 3) of the graphene–MnO_2 hybrid material. The N_2 adsorption–desorption isotherms show typical II/IV characteristic, and the corresponding specific surface area is about 123 $m^2\,g^{-1}$. Moreover, the pores constructed by the graphene nanosheets and manganese oxide nanosheets are mainly mesopores with a narrow pore size distribution of 2.0–7.7 nm and an average pore size of about 3.7 nm. In general, the size range of the hydrated ions in the electrolyte is typically 0.6–0.76 nm. For faradic pseudocapacitance, the minimum effective pore size should be bigger than 0.8 nm, while the minimum effective pore size should be greater than 1.2 nm for electric double-layer capacitance [35]. It is known that hydrated ions in the larger pores (>5 nm) are usually loosely bound to the surface layer and do not particularly contribute to the electric double-layer capacitance [36]. Therefore, the pore size at the range of 0.8–5 nm is the effective one required to increase either the pseudocapacitance or electric double-layer capacitance. The obtained material with high specific surface area and mesopores is favorable for improving both the main pseudocapacitance of layered MnO_2 and the electric double-layer capacitance of graphene since the hydrated ions in the electrolyte are easily accessible to the exterior and interior pore surfaces.

An asymmetric electrochemical capacitor based on the graphene–MnO_2 hybrid material as the positive electrode and graphene as the negative electrode using a 1 M Na_2SO_4 solution as electrolyte is assembled. To avoid the damage of the cell under high-voltage level during early cycles, it is necessary to polarize each electrode at the same potential and thus to estimate the stable electrochemical windows before cycling the hybrid cell [37]. At a fully reduced state, graphene gives about −0.9 V vs. SCE (Fig. S2a), but graphene–MnO_2 gives about 0.8 V vs. SCE (Fig. S2b) in the fully oxidized state. Thus, the potential of the asymmetric unit cell can reach 1.7 V in the fully charged state. The cyclic voltammetry (CV) curve of the asymmetric electrochemical capacitor with a voltage of 1.7 V at a scan rate of 10 mV s^{-1} shows rectangular mirror image with respect to the zero-current line, indicating relatively ideal capacitor behavior in a neutral aqueous electrolyte (Fig. 4a). Meanwhile, the curve shows no peak in the range between 0 and 1.7 V, indicating that the electrochemical capacitor is almost charged and discharged at a pseudoconstant rate over the complete voltammetric cycle [21]. The galvanostatic charge–discharge curves of the asymmetric electrochemical capacitor at different current densities show that the potentials of charge–discharge lines are nearly proportional to the charge or discharge time in the Na_2SO_4 electrolyte, indicating a rapid *I–V* response (Fig. 4b). On the other hand, the capacitor behavior of the asymmetry electrochemical capacitor is not ideal in comparison with the results reported by references [10,25], it is probably caused by the electrochemical adsorption/absorption or redox reactions at the interfaces between electrodes and electrolyte.

The cycle stability of the asymmetrical electrochemical capacitor is evaluated by repeating the galvanostatic charge–discharge test at the constant current density of 2230 mA g^{-1} between 0 and 1.7 V for 10,000 cycles (Fig. 4c). After 10,000 cycles, the asymmetry electrochemical capacitor retains about 69% of the initial capacitance. This cycling performance is prior to some other asymmetrical electrochemical capacitors, such as α-MnO_2–graphene//graphene electrochemical capacitor in Na_2SO_4 solution (79% retention after 1000 cycles) [25], AC//MnO_2 electrochemical capacitor in KOH (20% retention after 1500 cycles) [6], AC//MnO_2 electrochemical capacitor without N_2 bubbling (53% retention after 5000 cycles) [38], and multiwalled carbon nanotubes (MWCNTs)//MnO_2/MWCNT composite (72.3% retention after 300 cycles) [17]. These results demonstrate that the as-prepared sample, as an active electrode material, is very stable during the cycling test. Fig. 4d shows Ragone plot relative to the corresponding energy and power densities with current densities of 223–2230 mA g^{-1}. Graphene//graphene and graphene–MnO_2//graphene–MnO_2 symmetric electrochemical capacitors are tested galvanostatically between 0 and 1.0 V for comparison. It is worth noting that the maximum energy density obtained for asymmetric electrochemical capacitor with a cell voltage of 1.7 V is 21.27 Wh kg^{-1}, which is much higher than those of symmetric graphene//graphene electrochemical capacitor (3.15 Wh kg^{-1}) and graphene–MnO_2//graphene–MnO_2 electrochemical capacitor (7.64 Wh kg^{-1}). This value is higher than those of other reported symmetrical electrochemical capacitors [6], and also higher than those of other MnO_2-based asymmetric electrochemical capacitors with aqueous electrolyte solutions, such as AC//MnO_2 electrochemical capacitor (17.3 Wh kg^{-1}), Fe_3O_4//MnO_2 electrochemical capacitor (8.1 Wh kg^{-1}) [16], polyaniline//MnO_2 electrochemical capacitor (5.86 Wh kg^{-1}), polypyrrole//MnO_2 electrochemical capacitor (7.37 Wh kg^{-1}), poly (3,4-ethylenedioxythiophene)//MnO_2 electrochemical capacitor (13.5 Wh kg^{-1}) [39], and AC//$NaMnO_2$ electrochemical capacitor (19.5 Wh kg^{-1}) [40]. Moreover, the asymmetrical electrochemical capacitor still shows a high energy density of 10.03 Wh kg^{-1} even at an average power density of 2.53 kW kg^{-1}. These results suggest that the graphene–MnO_2 hybrid material is a very promising electrode material for fabricating electrochemical capacitors with both high energy and power densities.

The alternating current impedance of the asymmetric electrochemical capacitor for the first and the 10,000th cycles with a frequent range of 100 kHz to 0.1 Hz is shown in Fig. 5. The two Nyqusit plots are similar to each other in shape, namely one semicircle at high-frequency range (inserted in Fig. 5) and a nearly straight line at low-frequency range. After 10,000 cycles, two obvious characteristics of the Nyqusit plot can be observed, one is the electrochemical capacitor resistance increases from an initial value of 1.2 to 2.2 Ω, and the other is the semicircle becomes more obvious. These results suggest that the resistance of the electrodes and charge-transfer resistance increase. The higher the charge-transfer resistance, the lower the specific capacitance of the electrochemical capacitor [41]. The electrochemical capacitor has a higher charge-transfer resistance after 10,000 cycles, reflecting a lower specific capacitance. This change is probably attributed to the loss of adhesion of some active material with the current collector or the dissolution of some MnO_2. In addition, both the real and imaginary part of impedance for the 10,000th cycles are larger than that of the first cycle at low-frequency range, suggesting bigger diffusion impedance after 10,000 cycles, which is attributed to the increased diffusion and migration pathways of electrolyte ions during the charge–discharge process [26].

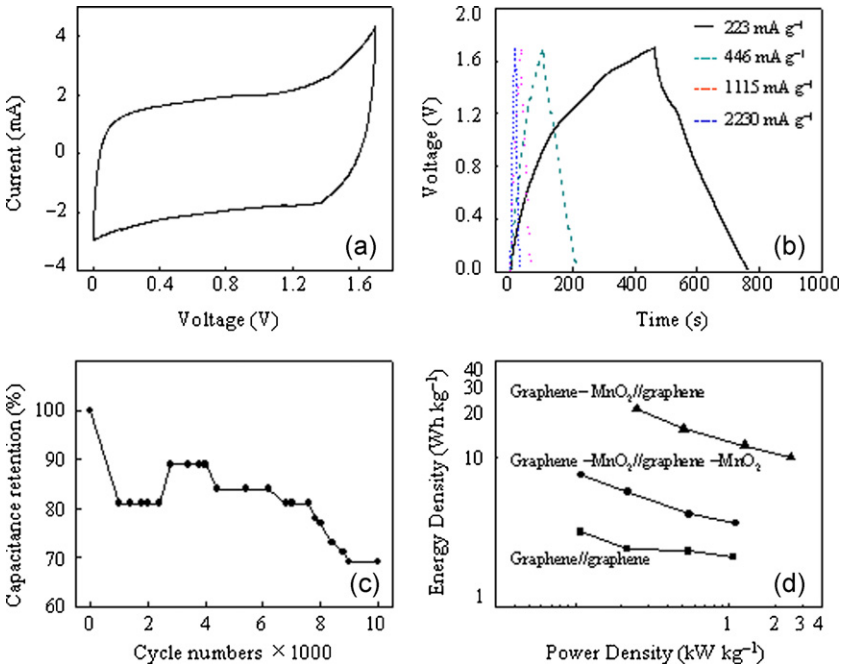

Fig. 4. CV curve of asymmetry electrochemical capacitor with a voltage of 1.7 V at a scan rate of 10 mV s^{-1} (a), galvanostatic charge–discharge profile of the asymmetric electrochemcial capacitor at different current densities (b), cycle performance of the asymmetry electrochemical capacitor with a voltage of 1.7 V at a current density of 2230 mA g^{-1} (c), and the Ragone plot related to energy and average power densities of the asymmetry electrochemical capacitor, graphene//graphene and graphene–MnO_2//graphene–MnO_2 symmetric electrochemical capacitor with a voltage of 1.0 V (d).

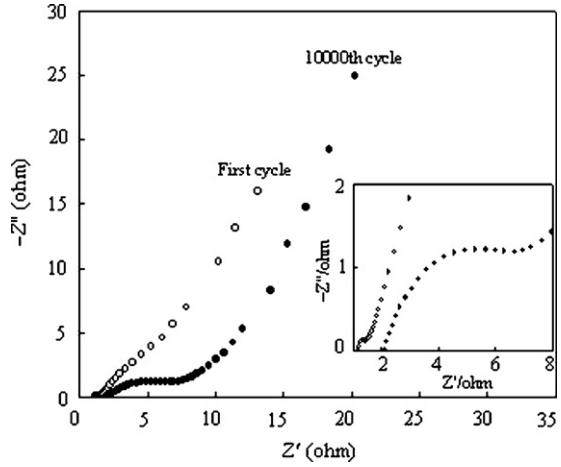

Fig. 5. The Nyquist plots of the experimental impedance for the asymmetry electrochemical capacitor during the cycle life test with a frequent range of 100 kHz to 0.1 Hz.

4. Conclusion

In conclusion, graphene–MnO_2 hybrid material has been synthesized by solution-phase assembly of aqueous dispersions of graphene nanosheets and manganese oxide nanosheets at room temperature. An asymmetrical electrochemical capacitor based on the graphene–MnO_2 hybrid material as positive electrode and graphene as the negative electrode is assembled with 1 M Na_2SO_4 solution as the electrolyte. The asymmetrical electrochemical capacitor can cycle reversibly in a voltage of 0–1.7 V and give a high energy density of 21.27 Wh kg^{-1}, which is much higher than those of symmetric electrochemical capacitors based on graphene and graphene–MnO_2. Moreover, it exhibits a high energy density of 10.03 Wh kg^{-1} even at an average power density of 2.53 kW kg^{-1} and presents an acceptable cycling performance after repeating the galvanostatic charge–discharge test at the constant current density of 2230 mA g^{-1} for 10,000 cycles. Therefore, the graphene–MnO_2 hybrid material is suitable and promising electrode material for electrochemical capacitors with high power and energy densities.

Acknowledgments

This work was supported by the National Natural Science Foundation of China (20971082) and the Fundamental Research Funds for the Central Universities (2010ZYGX022).

Appendix A. Supplementary data

Supplementary data associated with this article can be found, in the online version, at doi:10.1016/j.jpowsour.2011.09.005.

References

[1] Z. Chen, Y. Qin, D. Weng, Q. Xiao, Y. Peng, X. Wang, H. Li, F. Wei, Y. Lu, Adv. Funct. Mater. 19 (2009) 3420–3426.
[2] M. Winter, R. Brodd, Chem. Rev. 104 (2004) 4245–4269.
[3] A. Burke, J. Power Sources 91 (2000) 37–50.
[4] K.-H. Chang, C.-C. Hu, C.-M. Huang, Y.-L. Liu, C.-I. Chang, J. Power Sources 196 (2011) 2387–2392.
[5] G.-W. Yang, C.-L. Xu, H.-L. Li, Chem. Commun. 48 (2008) 6537–6539.
[6] D.-W. Wang, F. Li, M. Liu, G. Lu, H.-M. Cheng, Angew. Chem. Int. Ed. 47 (2008) 373–376.
[7] P. Simon, Y. Gogotsi, Nat. Mater. 7 (2008) 845–854.
[8] H. Wang, Q. Hao, X. Yang, L. Lu, X. Wang, Electrochem. Commun. 11 (2009) 1158–1161.
[9] S.-L. Chou, J.-Z. Wang, S.-Y. Chew, H.-K. Liu, S.-X. Dou, Electrochem. Commun. 10 (2008) 1724–1727.
[10] P.-J. Hung, K.-H. Chang, Y.-F. Lee, C.-C. Hu, K.-M. Lin, Electrochim. Acta 55 (2010) 6015–6021.
[11] W. Wei, X. Cui, W. Chen, D.G. Ivey, Chem. Soc. Rev. 40 (2011) 1697–1721.
[12] C.-C. Hu, C.-Y. Hung, K.-H. Chang, Y.-L. Yang, J. Power Sources 196 (2011) 847–850.
[13] C. Portet, P. Taberna, P. Simon, E. Flahaut, J. Electrochem. Soc. 153 (2006) A649–A653.
[14] T. Brousse, P.-L. Taberna, O. Crosnier, R. Dugas, P. Guillemet, Y. Scudeller, Y. Zhou, F. Favier, D. Bélanger, P. Simon, J. Power Sources 173 (2007) 633–641.

[15] Q. Qu, Y. Shi, L. Li, W. Guo, Y. Wu, H. Zhang, S. Guan, R. Holze, Electrochem. Commun. 11 (2009) 1325–1328.
[16] T. Cottineau, M. Toupin, T. Delahaye, T. Brousse, D. Bélanger, Appl. Phys. A 82 (2006) 599–606.
[17] H.-Q. Wang, Z.-S. Li, Y.-G. Huang, Q.-Y. Li, X.-Y. Wang, J. Mater. Chem. 20 (2010) 3883–3889.
[18] A. Yuan, Q. Zhang, Electrochem. Commun. 8 (2006) 1173–1178.
[19] T. Brousse, M. Toupin, D. Bélanger, J. Electrochem. Soc. 151 (2004) A614–A622.
[20] X. Du, C. Wang, M. Chen, Y. Jiao, J. Wang, J. Phys. Chem. C 113 (2009) 2643–2646.
[21] D.-W. Wang, F. Li, H.-M. Cheng, J. Power Sources 185 (2008) 1563–1568.
[22] A.K. Geim, Science 324 (2009) 1530–1534.
[23] Z. Li, J. Wang, S. Liu, X. Liu, S. Yang, J. Power Sources (2010), doi:10.1016/j.jpowsour.2011.05.036.
[24] S. Biswas, L. Drzal, Chem. Mater. 22 (2010) 5667–5671.
[25] Z.-S. Wu, W. Ren, D.-W. Wang, F. Li, B. Liu, H.-M. Cheng, ACS Nano 4 (2010) 5835–5842.
[26] J. Yan, Z. Fan, T. Wei, W. Qian, M. Zhang, F. Wei, Carbon 48 (2010) 3825–3833.
[27] Q. Cheng, J. Tang, J. Ma, H. Zhang, N. Shinya, L.-C. Qin, Carbon 49 (2011) 2917–2925.
[28] K.-H. Chang, Y.-F. Lee, C.-C. Hu, C.-I. Chang, C.-L. Liu, Y.-L. Yang, Chem. Commun. 46 (2010) 7957–7959.
[29] Z.-H. Liu, X. Yang, Y. Makita, K. Ooi, Chem. Mater. 14 (2002) 4800–4806.
[30] L. Wang, Y. Omomo, N. Sakai, K. Fukuda, I. Nakai, Y. Ebina, K. Takada, M. Watanabe, T. Sasaki, Chem. Mater. 15 (2003) 2873–2878.
[31] X. Zhang, W. Yang, D. Evans, J. Power Sources 184 (2008) 695–700.
[32] N. Kovtyukhova, P. Ollivier, B. Martin, T. Mallouk, S. Chizhik, E. Buzaneva, A. Gorchinskiy, Chem. Mater. 11 (1999) 771–779.
[33] Q. Feng, E.-H. Sun, K. Yanagisawa, N. Yamasaki, J. Ceram. Soc. Jpn. 105 (1997) 564–568.
[34] G. Wang, J. Yang, J. Park, X. Gou, B. Wang, H. Liu, J. Yao, J. Phys. Chem. C 112 (2008) 8192–8195.
[35] L. Cao, M. Lu, H.-L. Li, J. Electrochem. Soc. 152 (2005) A871–A875.
[36] K. An, W. Kim, Y. Park, Y. Choi, S. Lee, D. Chung, D. Bae, S. Lim, Y. Lee, Adv. Mater. 13 (2001) 497–500.
[37] M. Xu, L. Kong, W. Zhou, H. Li, J. Phys. Chem. C 111 (2007) 19141–19147.
[38] V. Khomenko, E. Raymundo-Piñero, F. Béguin, J. Power Sources 153 (2006) 183–190.
[39] V. Khomenko, E. Raymundo-Piñero, E. Frackowiak, F. Béguin, Appl. Phys. A 82 (2006) 567–573.
[40] Q. Qu, Y. Shi, S. Tian, Y. Chen, Y. Wu, R. Holze, J. Power Sources 194 (2009) 1222–1225.
[41] M.-S. Wu, C.-Y. Huang, K.-H. Lin, J. Power Sources 186 (2009) 557–564.